Diagnostic and Interventional Imaging (2019) **100**, 295—302

ORIGINAL ARTICLE /*Musculoskeletal imaging*

Comparison of bone lesion distribution between prostate cancer and multiple myeloma with whole-body MRI

A. Larbi[a], **P. Omoumi**[b], **V. Pasoglou**[a], **N. Michoux**[a], **P. Triqueneaux**[a], **B. Tombal**[c], **C. Cyteval**[d], **F.E. Lecouvet**[a,*]

[a] *Department of Radiology, Institut de Recherche expérimentale et Clinique (IREC), cliniques Universitaires Saint Luc, Université Catholique de Louvain (UCLouvain), 1200 Brussels, Belgium*
[b] *Department of Diagnostic and Interventional Radiology, Lausanne University Hospital, 1011 Lausanne, Switzerland*
[c] *Division of Urology, IREC, Cliniques Universitaires Saint Luc, UCLouvain, 1200 Brussels, Belgium*
[d] *Department of Radiology, Faculté de Médecine de Montpellier/Nîmes, Hôpital Lapeyronie, 34000 Montpellier, France*

KEYWORDS
Magnetic resonance imaging (MRI);
Whole-body MRI;
Prostate cancer;
Multiple myeloma

Abstract
Purpose: To assess the distribution of bone lesions in patients with prostate cancer (PCa) and those with multiple myeloma (MM) using whole-body magnetic resonance imaging (MRI); and to assess the added value of four anatomical regions located outside the thoraco-lumbo-pelvic area to detect the presence of bone lesions in a patient-based perspective.
Materials and methods: Fifty patients (50 men; mean age, 67 ± 10 [SD] years; range, 59—87 years) with PCa and forty-seven patients (27 women, 20 men; mean age, 62.5 ± 9 [SD] years; range, 47—90 years) with MM were included. Three radiologists assessed bone involvement in seven anatomical areas reading all MRI sequences.
Results: In patients with PCa, there was a cranio-caudal increasing prevalence of metastases (22% [11/50] in the humeri and cervical spine to 60% [30/50] in the pelvis). When the thoraco-lumbo-pelvic region was not involved, the prevalence of involvement of the cervical spine, proximal humeri, ribs, or proximal femurs was 0% in patients with PCa and ≥ 4% (except for the cervical spine, 0%) in those with MM.

* Corresponding author.
E-mail address: frederic.lecouvet@uclouvain.be (F.E. Lecouvet).

https://doi.org/10.1016/j.diii.2018.12.005

Conclusion: In patients with PCa, there is a cranio-caudal positive increment in the prevalences of metastases and covering the thoraco-lumbo-pelvic area is sufficient to determine the metastatic status of a patient with PCa. In patients with MM, there is added value of screening all regions, except the cervical spine, to detect additional lesions.

The ability to accurately detect bone involvement has a major importance in patients with ''osteophilic'' cancers like breast or prostate cancer (PCa) and in hematologic malignancies involving bones, like multiple myeloma (MM). Indeed, the detection of bone metastases (BM) or focal osteolytic lesions in MM, at the time of diagnosis or during the follow-up, has an impact on patient management. Most frequently, the presence of bone lesions leads to the introduction or adaptation of systemic therapy [1,2] or more specific treatments [3—7].

In patients with cancers at risk for skeletal dissemination, the search for BM has been performed for decades using bone scintigraphy (BS) [1]. In patients with MM, the radiographic skeletal survey has been used to detect characteristic lytic bone lesions [8]. However, whole-body magnetic resonance imaging (MRI) allows now coverage of the whole skeleton similar to BS and radiographic skeletal survey, and has several advantages [9—12].

In PCa, whole-body MRI has proven superior to BS and targeted radiographs for the staging and monitoring of BM. It represents, along with PSMA-ligand positron emission tomography and other specific tracers, the current imaging of choice in patients with PCa [13—16]. Whole-body MRI is superior to the radiographic skeletal survey for the detection of bone involvement in MM and is promoted as the first line imaging modality [17—21]. The protocols of whole-body MRI examinations have been defined, including anatomical T1 and STIR sequences, and more recently enriched with a systematic acquisition of diffusion-weighted images (DWI) as an adjunct to anatomical sequences [12,22].

The coverage of the whole-body with MRI results in long acquisition times (approximately 45 min), which is a limitation of this technique [23]. A limitation of skeletal coverage for BM and MM lesions to necessary and sufficient anatomical areas could help reduce examination times and optimize workflow, as access to MRI is critical in many countries [24].

The availability of whole-body MRI examinations acquired in metastatic cancers and in MM offers the opportunity of a critical approach of the technique and the possibility to determine the ''minimal'' anatomical areas to cover for an optimal skeletal screening. The need for covering the spine and pelvis as minimal MRI surveys (''axial skeleton'' approach) is well established for PCa and MM [19,21,25]. The specific diagnostic interest of other skeletal areas included in whole-body MRI surveys remains unclear. Based on previous data from the literature on the distribution of PCa and MM bone lesions, we hypothesized that minimal examination should include the thoraco-lumbo-pelvic region, and decided to investigate which additional anatomical areas should be included for optimal bone screening.

The purposes of this study were (1) to assess the distribution of bone marrow lesions in PCa and MM patients in seven anatomical regions; (2) to assess the added value of the four anatomical regions located outside the thoraco-lumbo-pelvic area to detect the presence of lesions in the perspective of a patient-based analysis. To achieve this, we determined the confidence intervals (CI) for the frequency of involvement of these four regions when the thoraco-lumbo-pelvic regions were not involved.

Materials and methods

Patients

This two-center study was approved by our institution's ethics committee, which did not require signed informed consent for the retrospective review of prospectively acquired data. Over a one year period, 50 consecutive patients with PCa at high risk for metastasis (newly diagnosed cancer with $\geq$ 20 ng/mL prostate-specific antigen (PSA), Gleason score $\geq$ 8, Union for International Cancer Control (UICC) clinical T stage 3 or 4; or suspicion of biochemical recurrence with a PSA doubling time $\leq$ 12 months) [26—29] were prospectively enrolled at the Cliniques Universitaires Saint Luc, Brussels, Belgium. During the same period, 47 patients with newly diagnosed and histologically proven MM were prospectively enrolled at the Lapeyronie Hospital, Montpellier, France. All 97 patients were examined using a whole-body MRI protocol as described below.

Bone marrow involvement

Three fellowship-trained musculoskeletal radiologists with 8-, 12-, and 25-years of experience each in oncologic imaging, including whole-body MRI, performed all readings together. The presence of bone lesions was determined based on the consensus reading of all morphologic and functional whole-body MRI sequences, and on the evaluation of all clinical, biological, histological and imaging data available at baseline and 6-months follow-up as part of the standard of care in our institutions. In PCa patients, available routine examinations consisted in ^{99m}technetium BS performed to detect bone metastases, complemented with targeted radiographs on equivocal foci with increased

uptake at BS considered as equivocal, and abdominopelvic computed tomography (CT) performed for lymph node detection [14,30]. In MM patients, the routine work-up consisted in a radiographic skeletal survey covering the skull, thoracic cage, cervical, thoracic and lumbar segments of the spine, both humeri and both femurs.

MRI protocol

The MRI studies were performed on two different 1.5-T MR magnets (PCa cohort: Achieva®, Philips Medical Systems; MM cohort: Magnetom Avanto®, Siemens Healthineers). Patients were placed on the imaging table headfirst in supine position and covered with head, neck, and spine coils and two 6-element body matrix coils. Five stacks of coronal T1 and STIR images and axial high b value DWI MR images were reconstructed and fused into one single stack of coronal whole-body images. The imaging parameters are detailed in Table 1 and elsewhere [31]. All images were read on PACS workstations (Carestream Vue; Carestream Health).

MRI readings

The presence of bone lesions was assessed at MRI, recorded in a per-region approach (distribution), and summarized in a per-patient approach (bone lesions present or absent). In each region, the bone marrow was considered as being either normal or as presenting one of three well-defined patterns of tumor involvement (focal, diffuse, and variegated; the latter being observed in patients with MM only). This widely accepted categorization has been repeatedly described [14,32—35]. Focal lesions were recorded if presenting a minimal diameter of 10 mm, corresponding to twice the slice thickness, to avoid partial-volume artifacts, as previously recommended [36].

Lesion distribution

The skeleton was divided into seven anatomical areas for evaluating the distribution of lesions: thoracic cage (including scapula, ribs and sternum), right and left humeri, cervical spine, thoracic spine, lumbar spine, bony pelvis, and right and left proximal femurs. Each region was considered involved if at least one focal lesion, or diffuse bone marrow involvement (including salt and pepper pattern at MRI) was present at imaging and confirmed on the rest of the clinico-biological-histological data.

Statistical analysis

With respect to lesion distribution, the frequency of involvement of the seven anatomical areas was determined in PCa and in MM patients. The frequencies of involvement along with their 95% confidence intervals (CI) of the humeri, thoracic cage, humeri and cervical spine was then determined in patients with no involvement of the thoraco-lumbo-pelvic region. Statistical analyses were performed using MedCalc Statistical Software version 17.2 (MedCalc Software bvba; https://www.medcalc.org; 2017).

Results

Patient population and frequency of bone involvement at whole-body MRI

Fifty patients with PCa at high risk for metastasis were enrolled (50 men; mean age, 67 ± 10 [SD] years; range, 59—87 years). Forty patients had been newly diagnosed with high-risk disease and 10 patients had PSA recurrence after radical treatment or when receiving androgen-deprivation therapy. Forty-seven patients with histologically proven, newly diagnosed MM were enrolled (27 women and 20 men; mean age, 62.5 ± 9 [SD] years; range, 47—90 years).

Thirty-eight of the 50 PCa patients (38/50; 76%) had bone metastases on whole-body MRI. Of these 38 patients, 34 patients (34/38; 89%) had focal lesions and 4 patients (4/38; 11%) had diffuse bone marrow infiltration. Thirty-one of 47 MM patients (66%) had bone marrow involvement on whole-body MRI. Among these patients, 23 patients (74%) had focal lesions, 5 patients (16%) had diffuse bone marrow involvement, and 3 patients (10%) presented a salt-and-pepper infiltration of the bone marrow.

Distribution of lesions

In patients with PCa, the most frequently involved areas were the pelvis (30/50; 60%), followed by the lumbar spine (25/50; 50%), and thoracic spine (22/50; 44%) (Table 2). There was a ''cranio-caudal positive gradient'' in the frequencies of metastatic involvement ranging from 22% of bone involvement in the humeri and the cervical spine, to 60% in the pelvis (Fig. 1). In the MM population, the distribution of lesions ranged from 15% (7/47; cervical spine) to 34% (16/47; pelvis) without evident cranio-caudal gradient (Fig. 2).

Involvement of anatomical areas outside the thoraco-lumbo-pelvic region

For patients with PCa, when the thoraco-lumbo-pelvic region was not involved, the frequencies of involvement of cervical spine, proximal humeri, ribs, and proximal femurs were all 0% (95% CI = 0.0—7.4%) (Table 3). For patients with MM, when the thoraco-lumbo-pelvic region was not involved, the frequencies of involvement ranged from 0% (0/47) to 11% (5/47). Of note, no cervical spine involvement was found in patients free of thoraco-lumbar spine involvement, for both patients with PCa and those with MM.

Discussion

This study compared the skeletal distribution of neoplastic bone marrow lesions between patients with PCa and those with MM. We also evaluated the necessary skeletal coverage for a confident detection of bone involvement in both diseases in a patient-based approach (positive/negative for bone involvement). Regarding lesion distribution, a substantial difference is worth noting: whereas bone marrow lesions are homogeneously spread over the different parts of the skeleton in patients with MM, bone metastases from PCa show an increasing frequency among the investigated

Table 1 MR imaging parameters.

Parameter	T1 (Siemens)	T1 (Philips)	STIR (Siemens)	STIR (Philips)	DWI (Siemens)	DWI (Philips)
Plane	Coronal	Coronal	Coronal	Coronal	Transverse	Transverse
Phase encoding direction	Right-left	Right-left	Feet-head	Feet-head	Anterior-posterior	Anterior-posterior
Field of view (mm)	265	265	265	265	265	265
Matrix	384 × 307	208 × 287	256 × 320	336 × 120	112 × 63	108 × 63
Slice thickness (mm)	4	4	4	4	5	5
Interslice gap (mm)	1	1	1	1	0	0
Number of slices	30	30	30	30	30	30
Number of averages	1	1	2	2	1	1
TR (ms)	550	537	3200	4358	3100	3134
TE (ms)	15	18	50	64	63	64
TSE factor	4	7	17	30	—	—
TI (ms)	—	—	150	150	150	150
Fat suppression technique	—	—	STIR	STIR	STIR	STIR
b-values (s/mm^2)	—	—	—	—	0—800	0—800
Acquisition time[a]	4 min 55 sec	4 min 5 sec	6 min 52 sec	6 min 30 sec	10 min 20 sec	10 min 25 sec

DWI: diffusion-weighted imaging; STIR: short tau inversion recovery; T1: T1-weighted sequence; TE: echo time; TI: inversion time; TR: repetition time; TSE: turbo spin echo.
[a] Time to image all stations for each sequence.

Table 2 Frequency of involvement of different anatomical regions in 50 patients with prostate cancer and in 47 patients with multiple myeloma.

	Prostate cancer	Multiple myeloma
Humeri	11/50 (22%) [11; 39]	7/47 (15%) [6; 31]
Ribs	15/50 (30%) [18; 52]	12/47 (26%) [13; 45]
Cervical spine	11/50 (22%) [11; 39]	7/47 (15%) [6; 31]
Thoracic spine	22/50 (44%) [28; 67]	13/47 (28%) [15; 47]
Lumbar spine	25/50 (50%) [32; 74]	12/47 (26%) [13; 45]
Pelvis	30/50 (60%) [41; 86]	16/47 (34.0%) [20; 55]
Proximal femurs	13/50 (26%) [14; 45]	10/47 (21%) [10; 39]
Total spine	29/50 (58%) [39; 83]	16/47 (34.0%) [20; 5]
Thoraco-lumbo-pelvic region	38/50 (76%) [54; 100]	21/47 (45%) [0; 68]
Thoraco-lumbo-pelvic region and proximal femurs	38/50 (76%) [54; 100]	23/47 (49%) [31; 73]

Data are proportions; raw data are followed by % in parentheses. Numbers in brackets are 95% CI.

anatomic areas in a cranio—caudal direction, with the thoracic and lumbar spine segments and bony pelvis being the most frequently affected areas.

Regarding the minimal anatomic coverage for the positive diagnosis of bone involvement in a given patient, the study of the thoraco-lumbo-pelvic area appears sufficient to detect the presence of bone metastases in PCa patients, with little added value for other anatomic areas. Conversely, coverage of the thoracic cage, humeri and femurs appears necessary for an optimal survey of bone involvement in MM patients. Coverage of the cervical spine seems to have no added value to detect bone marrow involvement in patients, both in PCa and in MM patients. This finding may be of interest given the frequent poor quality and difficult analysis of cervical region images with whole-body MRI. In general, MRI has shown lower diagnostic performances for the detection of cervical spine metastases compared to other locations in the spine [37]. Of note, covering the femurs did not contribute to the detection of metastatic patients in PCa, whereas it was helpful in MM. Although proximal aspect of femurs is included in the coronal sequences obtained on the pelvis, this finding suggests that extensive cranio-caudal coverage of the femurs is not mandatory, which could contribute to shortening the examination durations, especially in larger patients.

The cranio-caudal increment in the prevalence of bone marrow lesions and the predominant involvement of the thoraco-lumbo-pelvic area has already be pointed out in PCa, both in autopsy and imaging studies, contrasting with the more homogeneous distribution of metastases of other solid cancers and MM lesions. Bubendorf et al. in an autopsy study of 1509 PCa patients, reported skeletal metastases in 90% of cases, and noted a decreasing prevalence of lesions from the lumbar (97%) to the cervical (38%) segments of the spine [38]. Other autopsy studies also pointed out the spine and bony pelvis as the most frequently involved skeletal

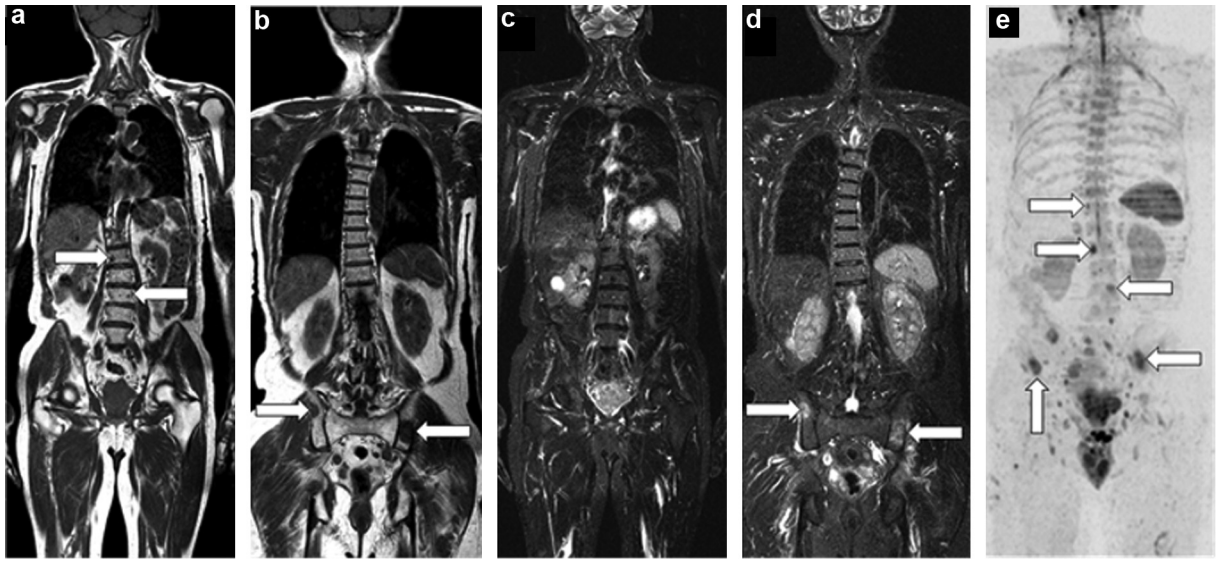

Figure 1. Whole-body MR examination in a 55-year-old man with newly diagnosed prostate cancer reveals lumbo-pelvic distribution of metastases. (a) Coronal T1-weighted and (b) short tau inversion-recovery (STIR) images, and (c) reconstructed coronal maximal intensity projection view from diffusion-weighted imaging sequence (inverted grayscale, b = 800 s/·mm^{-2}) show multiple areas typical for bone metastases (arrows). Note their predominant lumbo-pelvic location.

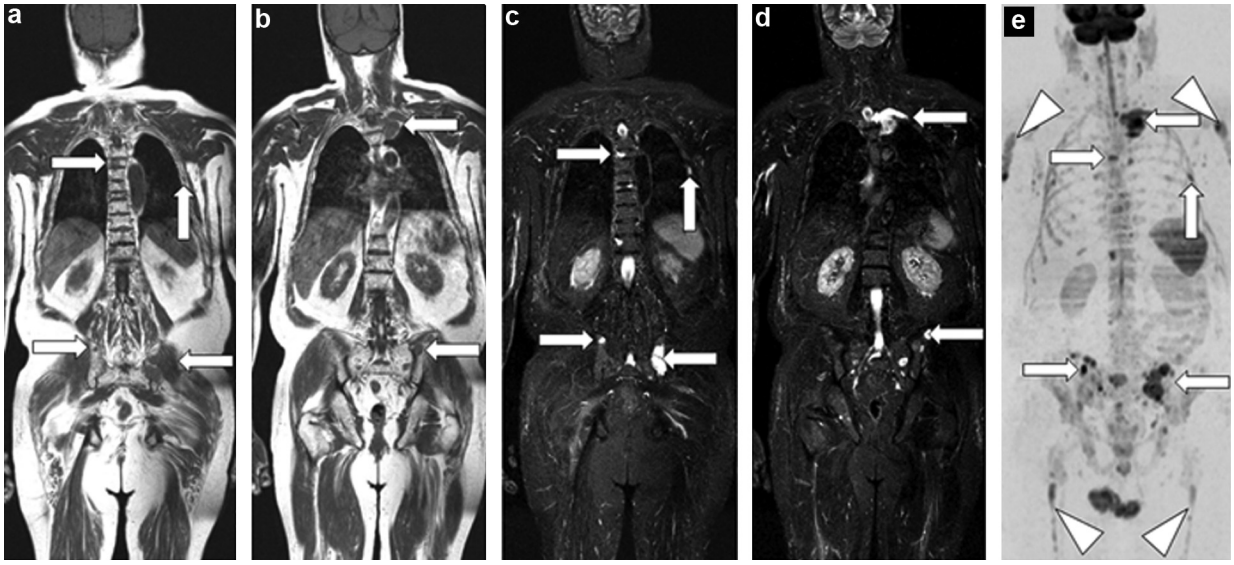

Figure 2. Whole-body MRI examination in a 74-year-old man with newly diagnosed multiple myeloma reveals homogeneous spread of bone marrow lesions along the whole axial skeleton. (a) Coronal T1-weighted and (b) STIR images, and (c) reconstructed coronal maximal intensity projection view from diffusion-weighted images DWI (inverted grayscale, b = 800 s/·mm^{-2}) show multiple areas of low signal typical for myeloma foci (arrows). There is no clear preferential distribution within the skeleton, and in particular no predominant lumbo-pelvic distribution. Note the involvement of thoracic spine and ribs. Note also the involvement of femurs and humeri (arrowheads).

areas [39,40]. Previous imaging studies, using either NaF PET(CT), BS, SPECT, or whole-body MRI found the same thoraco-lumbar and pelvic predominant distribution of bone metastases from PCa [36,41,42].

PCa can theoretically disseminate either through prostatic veins or the lymphatics. The disease may involve the lower spine and pelvis via regional lymph nodes. But the most likely predominant hypothesis to explain the preferential involvement of the lower thoracic and lumbar spine and of the pelvi-femoral area by PCa metastases has been proposed decades ago and is known as the ''Batson theory'' [43]. This theory highlighted the key role played by a valveless venous system extensively developed along the vertebral column up to the skull and featuring rich anastomoses between the veins of the pelvic viscera, the veins in the spinal canal, and the intercostal veins, communicating with the azygous veins, and from there with the bronchial veins. Hence, this system allows metastatic seeding bypassing the caval venous system and pulmonary circulation. The valveless nature of the system explains the retrograde migration of neoplastic cells in the venous flow from the pelvic veins to this system in relation with variations in

Table 3 Proportions of tumors in region 1 when region 2 was free of tumors.

Region 1	Region 2	Prostate cancer	Multiple myeloma
Humeri	Thoraco-lumbo-pelvic region	0/50 (0%) [0; 7]	3/47 (6%) [0; 12]
Proximal femurs	Thoraco-lumbo-pelvic region	0/50 (0%) [0; 7]	2/47 (4%) [0; 15]
Ribs	Thoraco-lumbo-pelvic region	0/50 (0%) [0; 7]	2/47 (4%) [4; 8]
Cervical spine	Thoraco-lumbo-pelvic region	0/50 (0%) [0; 7]	0/47 (0%) [0; 8]
Thoracic spine	Lumbar spine	3/50 (6%) [1; 17]	5/47 (11%) [3; 24]

Data are proportions; raw data are followed by % in parentheses. Numbers in brackets are 95% CI.

abdominal pressures (during straining, coughing or lifting for example) [43].

The predominant involvement of the thoraco-lumbo-pelvic area in PCa patients parallels the results of previous studies on MRI screening and coming to the conclusion that a limited MRI marrow screen confined to the axial skeleton (i.e., the thoraco-lumbar spine and pelvi-femoral area) would be sufficient for bone screening and would not result in any significant loss of accuracy for staging compared with BS or with whole-body MRI surveys, as isolated peripheral skeletal metastases without involvement of the thoraco-lumbar spine and pelvi-femoral area were almost never observed in these studies [25,36].

Promoting MRI surveys limited to the thoraco-lumbo-pelvic area, might be regarded as ''outdated'', when whole-body MRI is available and is recommended in many studies, allowing for a concurrent bone and lymph node metastatic screening [9,14,44—46]. However, a thoraco-lumbo-pelvic MRI bone survey is limited to 15 minutes of magnet time, compared to the 45—50 minutes required for a whole-body MRI study. MRI surveys might be considered as a reliable triage tool to ''rule in'' metastatic disease in patients at high risk. The presence of polymetastatic disease in these areas would be sufficient to start therapy [47].

In our study, we found a more homogeneous distribution of MM lesions compared to PCa metastases. This is because MM is a disease that diffusely involves the red marrow-containing skeleton [48]. Extensive infiltration of the bone marrow by abnormal plasma cells is invariably seen at autopsy, including 15% of patients in whom no abnormality was seen on radiographic skeletal surveys [49]. The current study on MRI thus suggests that extensive body coverage is necessary to confidently identify bone involvement. This is in line with the previous demonstration that an MRI survey limited to the spine missed significant lesions compared to more exhaustive MRI coverage [50]. This also parallels the observation that spine and pelvis coverage using MRI was insufficient compared to whole-body radiographic skeletal survey given the high sensitivity of skull and ribs radiographs to detect osteolytic MM lesions [51]. Finally, our results support the whole-body MRI approach recommended by authorities in the field of MM and its preference over a limited spine and pelvic survey [19,21].

Our study has several limitations. First, the small number of patients needs further larger scale studies to validate our results. The lack of added value of including the cervical spine in both PCa and MM patients, as well as the ribs, proximal humeri and proximal femurs in PCa patients needs to be further confirmed. Second, we deliberately chose two different conditions to study the value of whole-body MRI in its two most validated indications. These findings should not be extrapolated to other cancers involving the skeleton [52,53]. A third limitation is the inclusion of patients at relatively early stages of skeletal dissemination so that our results might not be applied to patients with more advanced disease [54]. Finally, we did not obtain histological confirmation and positive findings were considered as bone metastases or MM foci at MRI [55].

In conclusion, our results suggest a cranio-caudal increase in the prevalence of bone metastases in PCa, whereas the distribution of lesions in MM is more homogeneous, with no gradient. The assessment of the axial skeleton using MRI (thoraco-lumbar spine and pelvis) is sufficient to detect bone metastases in PCa, whereas coverage of the entire axial skeleton with whole-body MRI seems necessary to detect MM involvement.

Disclosure of interest

The authors declare that they have no competing interest.

References

[1] Cornford P, Bellmunt J, Bolla M, Briers E, De Santis M, Gross T, et al. EAU-ESTRO-SIOG Guidelines on prostate cancer. Part II: treatment of relapsing, metastatic, and castration-resistant prostate cancer. Eur Urol 2017;71:630—42.

[2] Durie BG. The role of anatomic and functional staging in myeloma: description of Durie/Salmon plus staging system. Eur J Cancer 2006;42:1539—43.

[3] Coleman R, Body JJ, Aapro M, Hadji P, Herrstedt J. Bone health in cancer patients: ESMO Clinical Practice Guidelines. Ann Oncol 2014;25:124—37.

[4] Tosoian JJ, Gorin MA, Ross AE, Pienta KJ, Tran PT, Schaeffer EM. Oligometastatic prostate cancer: definitions, clinical outcomes, and treatment considerations. Nat Rev Urol 2017;14:15—25.

[5] deSouza NM, Liu Y, Chiti A, Oprea-Lager D, Gebhart G, Van Beers BE, et al. Strategies and technical challenges for imaging oligometastatic disease: recommendations from the European Organisation for Research and Treatment of Cancer imaging group. Eur J Cancer 2018;91:153—63.

[6] Lecouvet F, Oprea-Lager D, Liu Y, Ost P, Bidaut L, Collette L, et al. Use of modern imaging methods to facilitate trials of metastasis-directed therapy for oligometastatic disease in prostate cancer: a consensus recommendation from the EORTC Imaging Group. Lancet Oncol 2018;19:e534—45 https://doi.org/10.1016/S1470-2045(18)30571-0.

[7] Garnon J, Koch G, Caudrelier J, Tsoumakidou G, Cazzato RL, Gangi A. Expanding the borders: image-guided procedures for the treatment of musculoskeletal tumors. Diagn Interv Imaging 2017;98:635—44.
[8] Durie BG, Salmon SE. A clinical staging system for multiple myeloma. Correlation of measured myeloma cell mass with presenting clinical features, response to treatment, and survival. Cancer 1975;36:842—54.
[9] Lauenstein TC, Goehde SC, Herborn CU, Goyen M, Oberhoff C, Debatin JF, et al. Whole-body MR imaging: evaluation of patients for metastases. Radiology 2004;233:139—48.
[10] Messiou C, Kaiser M. Whole body diffusion weighted MRI-a new view of myeloma. Br J Haematol 2015;171:29—37.
[11] Gutzeit A, Doert A, Froehlich JM, Eckhardt BP, Meili A, Scherr P, et al. Comparison of diffusion-weighted whole body MRI and skeletal scintigraphy for the detection of bone metastases in patients with prostate or breast carcinoma. Skeletal Radiol 2010;39:333—43.
[12] Lecouvet FE. Whole-body MR imaging: musculoskeletal applications. Radiology 2016;279:345—65.
[13] Padhani AR, Koh DM, Collins DJ. Whole-body diffusion-weighted MR imaging in cancer: current status and research directions. Radiology 2011;261:700—18.
[14] Lecouvet FE, El Mouedden J, Collette L, Coche E, Danse E, Jamar F, et al. Can whole-body magnetic resonance imaging with diffusion-weighted imaging replace Tc 99m bone scanning and computed tomography for single-step detection of metastases in patients with high-risk prostate cancer? Eur Urol 2012;62:68—75.
[15] Tombal B, Lecouvet F. Modern detection of prostate cancer's bone metastasis: is the bone scan era over? Adv Urol 2012;2012:893193.
[16] Lecouvet FE, Larbi A, Pasoglou V, Omoumi P, Tombal B, Michoux N, et al. MRI for response assessment in metastatic bone disease. Eur Radiol 2013;23:1986—97.
[17] Walker R, Barlogie B, Haessler J, Tricot G, Anaissie E, ShaughnessyJr JD, et al. Magnetic resonance imaging in multiple myeloma: diagnostic and clinical implications. J Clin Oncol 2007;25:1121—8.
[18] Baur-Melnyk A, Buhmann S, Becker C, Schoenberg SO, Lang N, Bartl R, et al. Whole-body MRI versus whole-body MDCT for staging of multiple myeloma. AJR Am J Roentgenol 2008;190:1097—104.
[19] Dimopoulos MA, Hillengass J, Usmani S, Zamagni E, Lentzsch S, Davies FE, et al. Role of magnetic resonance imaging in the management of patients with multiple myeloma: a consensus statement. J Clin Oncol 2015;33:657—64.
[20] Rajkumar SV, Dimopoulos MA, Palumbo A, Blade J, Merlini G, Mateos MV, et al. International myeloma Working Group updated criteria for the diagnosis of multiple myeloma. Lancet Oncol 2014;15:e538—48.
[21] NICE guidelines, myeloma: diagnosis and management; 2016. https://www.nice.org.uk/guidance/ng35/chapter/Recommendations; (Accessed 18.12.18).
[22] Padhani AR, Lecouvet FE, Tunariu N, Koh DM, De Keyzer F, Collins DJ, et al. METastasis reporting and data system for prostate cancer: practical guidelines for acquisition, interpretation, and reporting of whole-body magnetic resonance imaging-based evaluations of multiorgan involvement in advanced prostate cancer. Eur Urol 2017;71:81—92.
[23] Adams HJ, Kwee TC, Vermoolen MA, Ludwig I, Bierings MB, Nievelstein RA. Whole-body MRI vs. CT for staging lymphoma: patient experience. Eur J Radiol 2014;83:163—6.
[24] Renard-Penna R, Rouviere O, Puech P, Borgogno C, Abbas L, Roy C, et al. Current practice and access to prostate MR imaging in France. Diagn Interv Imaging 2016;97:1125—9.
[25] Traill ZC, Talbot D, Golding S, Gleeson FV. Magnetic resonance imaging versus radionuclide scintigraphy in screening for bone metastases. Clin Radiol 1999;54:448—51.
[26] Tombal B, Alcaraz A, James N, Valdagni R, Irani J. Can we improve the definition of high-risk, hormone naive, non-metastatic prostate cancer? BJU Int 2014;113:189—99.
[27] Lecouvet FE, Geukens D, Stainier A, Jamar F, Jamart J, d'Othee BJ, et al. Magnetic resonance imaging of the axial skeleton for detecting bone metastases in patients with high-risk prostate cancer: diagnostic and cost-effectiveness and comparison with current detection strategies. J Clin Oncol 2007;25:3281—7.
[28] Heidenreich A, Bastian PJ, Bellmunt J, Bolla M, Joniau S, van der Kwast T, et al. EAU guidelines on prostate cancer. Part II: treatment of advanced, relapsing, and castration-resistant prostate cancer. Eur Urol 2014;65:467—79.
[29] Heidenreich A, Bastian PJ, Bellmunt J, Bolla M, Joniau S, van der Kwast T, et al. EAU guidelines on prostate cancer. Part 1: screening, diagnosis, and local treatment with curative intent-update 2013. Eur Urol 2014;65:124—37.
[30] Turner JW, Hawes DR, Williams RD. Magnetic resonance imaging for detection of prostate cancer metastatic to bone. J Urol 1993;149:1482—4.
[31] Larbi A, Omoumi P, Pasoglou V, Michoux N, Triqueneaux P, Tombal B, et al. Whole-body MRI to assess bone involvement in prostate cancer and multiple myeloma: comparison of the diagnostic accuracies of the T1, short tau inversion recovery (STIR), and high b-values diffusion-weighted imaging (DWI) sequences. Eur Radiol 2018, http://dx.doi.org/10.1007/s00330-018-5796-1.
[32] Padhani AR, Koh DM. Diffusion MR imaging for monitoring of treatment response. Magn Reson Imaging Clin N Am 2011;19:181—209.
[33] Koh DM, Blackledge M, Padhani AR, Takahara T, Kwee TC, Leach MO, et al. Whole-body diffusion-weighted MRI: tips, tricks, and pitfalls. AJR Am J Roentgenol 2012;199:252—62.
[34] Vanel D, Dromain C, Tardivon A. MRI of bone marrow disorders. Eur Radiol 2000;10:224—9.
[35] Baur-Melnyk A, Buhmann S, Durr HR, Reiser M. Role of MRI for the diagnosis and prognosis of multiple myeloma. Eur J Radiol 2005;55:56—63.
[36] Lecouvet FE, Simon M, Tombal B, Jamart J, Vande Berg BC, Simoni P. Whole-body MRI (WB-MRI) versus axial skeleton MRI (AS-MRI) to detect and measure bone metastases in prostate cancer (PCa). Eur Radiol 2010;20:2973—82.
[37] Maeder Y, Dunet V, Richard R, Becce F, Omoumi P. Bone marrow metastases: T2-weighted Dixon spin-echo fat images can replace T1-weighted spin-echo images. Radiology 2018;286:948—59.
[38] Bubendorf L, Schopfer A, Wagner U, Sauter G, Moch H, Willi N, et al. Metastatic patterns of prostate cancer: an autopsy study of 1589 patients. Hum Pathol 2000;31:578—83.
[39] Lamothe F, Kovi J, Heshmat MY, Green EJ. Dissemination of prostatic carcinoma: an autopsy study. J Natl Med Assoc 1986;78:1083—6.
[40] Mintz ERSG. Autopsy findings in 100 cases of prostatic cancer. N Engl J Med 1934;211:479—87.
[41] Mosavi F, Johansson S, Sandberg DT, Turesson I, Sorensen J, Ahlstrom H. Whole-body diffusion-weighted MRI compared with (18)F-NaF PET/CT for detection of bone metastases in patients with high-risk prostate carcinoma. AJR Am J Roentgenol 2012;199:1114—20.
[42] Even-Sapir E, Metser U, Mishani E, Lievshitz G, Lerman H, Leibovitch I. The detection of bone metastases in patients with high-risk prostate cancer: 99mTc-MDP Planar bone scintigraphy, single- and multi-field-of-view SPECT, 18F-fluoride PET, and 18F-fluoride PET/CT. J Nucl Med 2006;47:287—97.

[43] Batson OV. The function of the vertebral veins and their role in the spread of metastases. Ann Surg 1940;112:138—49.
[44] Freedman GM, Negendank WG, Hudes GR, Shaer AH, Hanks GE. Preliminary results of a bone marrow magnetic resonance imaging protocol for patients with high-risk prostate cancer. Urology 1999;54:118—23.
[45] Tombal B, Rezazadeh A, Therasse P, Van Cangh PJ, Vande Berg B, Lecouvet FE. Magnetic resonance imaging of the axial skeleton enables objective measurement of tumor response on prostate cancer bone metastases. Prostate 2005;65:178—87.
[46] Lauenstein TC, Freudenberg LS, Goehde SC, Ruehm SG, Goyen M, Bosk S, et al. Whole-body MRI using a rolling table platform for the detection of bone metastases. Eur Radiol 2002;12:2091—9.
[47] Gillessen S, Omlin A, Attard G, de Bono JS, Efstathiou E, Fizazi K, et al. Management of patients with advanced prostate cancer: recommendations of the St Gallen advanced prostate cancer consensus Conference (APCCC) 2015. Ann Oncol 2015;26:1589—604.
[48] Walker RC, Brown TL, Jones-Jackson LB, De Blanche L, Bartel T. Imaging of multiple myeloma and related plasma cell dyscrasias. J Nucl Med 2012;53:1091—101.
[49] Kapadia SB. Multiple myeloma: a clinicopathologic study of 62 consecutively autopsied cases. Medicine 1980;59:380—92.
[50] Bauerle T, Hillengass J, Fechtner K, Zechmann CM, Grenacher L, Moehler TM, et al. Multiple myeloma and monoclonal gammopathy of undetermined significance: importance of whole-body versus spinal MR imaging. Radiology 2009;252:477—85.
[51] Lecouvet FE, Malghem J, Michaux L, Maldague B, Ferrant A, Michaux JL, et al. Skeletal survey in advanced multiple myeloma: radiographic versus MR imaging survey. Br J Haematol 1999;106:35—9.
[52] Haubold-Reuter BG, Duewell S, Schilcher BR, Marincek B, von Schulthess GK. The value of bone scintigraphy, bone marrow scintigraphy and fast spin-echo magnetic resonance imaging in staging of patients with malignant solid tumours: a prospective study. Eur J Nucl Med 1993;20:1063—9.
[53] Cumming J, Hacking N, Fairhurst J, Ackery D, Jenkins JD. Distribution of bony metastases in prostatic carcinoma. Br J Urol 1990;66:411—4.
[54] Wang C, Shen Y, Zhu S. Distribution features of skeletal metastases: a comparative study between pulmonary and prostate cancers. PLoS One 2015;10:e0143437.
[55] Fujii Y, Higashi Y, Owada F, Okuno T, Mizuno H, Mizuno H. Magnetic resonance imaging for the diagnosis of prostate cancer metastatic to bone. Br J Urol 1995;75:54—8.